ADVANCED MATERIALS

Supporting Information

for *Adv. Mater.*, DOI: 10.1002/adma.201703026

Significant Performance Enhancement of Polymer Resins by Bioinspired Dynamic Bonding

*Sungbaek Seo, Dong Woog Lee, Jin Soo Ahn, Keila Cunha, Emmanouela Filippidi, Sung Won Ju, Eeseul Shin, Byeong-Su Kim, Zachary A. Levine, Roberto D. Lins, Jacob N. Israelachvili, J. Herbert Waite, Megan T. Valentine, Joan Emma Shea, and B. Kollbe Ahn**

Supporting Information

Significant performance enhancement of polymer resins by bioinspired dynamic bonding

Sungbaek Seo[†], Dong Woog Lee[†], Jin Soo Ahn[†], Keila Cunha[†], Emmanouela Filippidi, Sung Won Ju, Eeseul Shin, Byeong-Su Kim, Zachary A. Levine, Roberto D. Lins, Jacob N. Israelachvili, J. Herbert Waite, Megan T. Valentine, Joan Emma Shea, and B. Kollbe Ahn[*]

1. Materials

All reactions were carried out under argon unless otherwise noted. All glassware was pre-dried in an oven at 150 ^{o}C for 30 min. 1,8-Octanediol, acryloyl chloride, triethylamine, 3,4-dihydroxyhydrocinnamic acid, *N*,*N'*-dicyclohexylcarbodiimide (DCC), 4-(dimethylamino)pyridine (DMAP), tetrabutylammonium fluoride solution – 1 M in THF (TBAF), 3-(trimethoxysilyl)propyl acrylate, triethylene glycol dimethacrylate (TEGDMA), bisphenol A glycerolate dimethacrylate (Bis-GMA), 2-(dimethylamino)ethyl methacrylate (DMAEMA) and camphorquinone (CQ) were purchased from Sigma-Aldrich. Benzyl acrylate (P_1), 4-hydroxybenzyl alcohol, 10-methacryloyloxydecyl dihydrogen phosphate (MDP) and glass filler (2-8 μm) were purchased from Alfa Aesar, Chem-Impex International, Kuraray Medical Inc., and Youth Tech Co., respectively. Triethylsilane-protected eugenol acrylate was provided by Osaka Organic Chemical Industry LTD.

2. Synthesis of compounds

Bioinspired primer molecules (P_2-P_4) were synthesized (**Supplementary Fig. 1**). The chemical structure and mass was confirmed by ^{1}H NMR and Mass spectrometry.

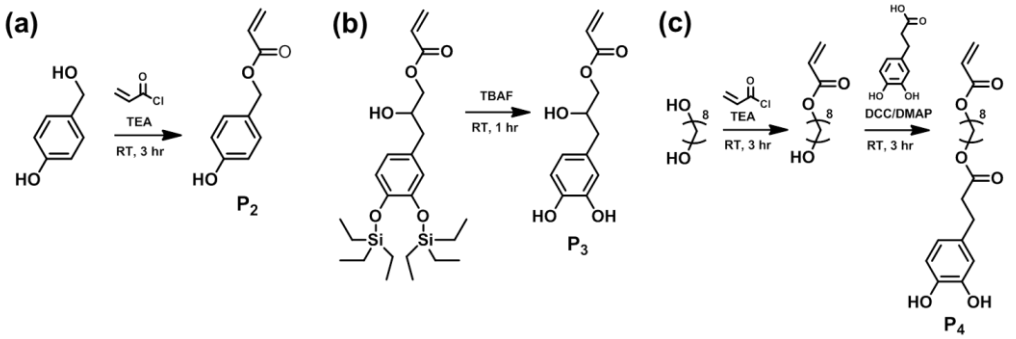

Supplementary Figure 1. Synthetic scheme of (a) 4-hydroxybenzyl acrylate (P_2), (b) 3-(3,4-dihydroxyphenyl)-2-hydroxypropyl acrylate (P_3), and (c) 8-((3-(3,4-dihydroxyphenyl)propanoyl)oxy)octyl acrylate (P_4).

4-Hydroxybenzyl acrylate (P_2). 4-Hydroxybenzyl alcohol (5 g, 40.28 mmol, 1.0 equiv) and triethylamine (6.7 ml, 48.33 mmol, 1.2 equiv) were agitated in THF (30 ml) at room temperature for 1 min. Subsequently, acryloyl chloride (3.27 ml, 40.28 mmol, 1.0 equiv) was added dropwise into the reaction mixture, and the reaction continued for 3 hours. The THF solvent was removed using a rotary vacuum evaporator. The crude material was extracted with 150 ml diethyl ether and the solution washed with 1N HCl. After purification by Biotage Isolera^{TM} Prime automatic column chromatography (Biotage SNAP 50 g silica column; hexane/diethyl ether 100 : 0 to 75 : 25 gradient; flow rate 40 ml/min), 3 g (42 % yield) of a transparent oil was obtained.

^{1}H NMR (600 MHz, DMSO-d_6): = 9.49 (s, 1H, Ar-O*H*), 7.18 (d, 2H, Ar-*H*), 6.72 (d, 2H, Ar-*H*), 6.28 (d, 1H, -CH=CH_2), 6.16 (q, 1H, -C*H*=CH_2), 5.91 (d, 1H, -CH=CH_2), 5.01 (s, 2H, -CH_2CH(OH)-) (**Supplementary Fig. 2**). EI-MS, m/z = 179.05 [M+Na^+].

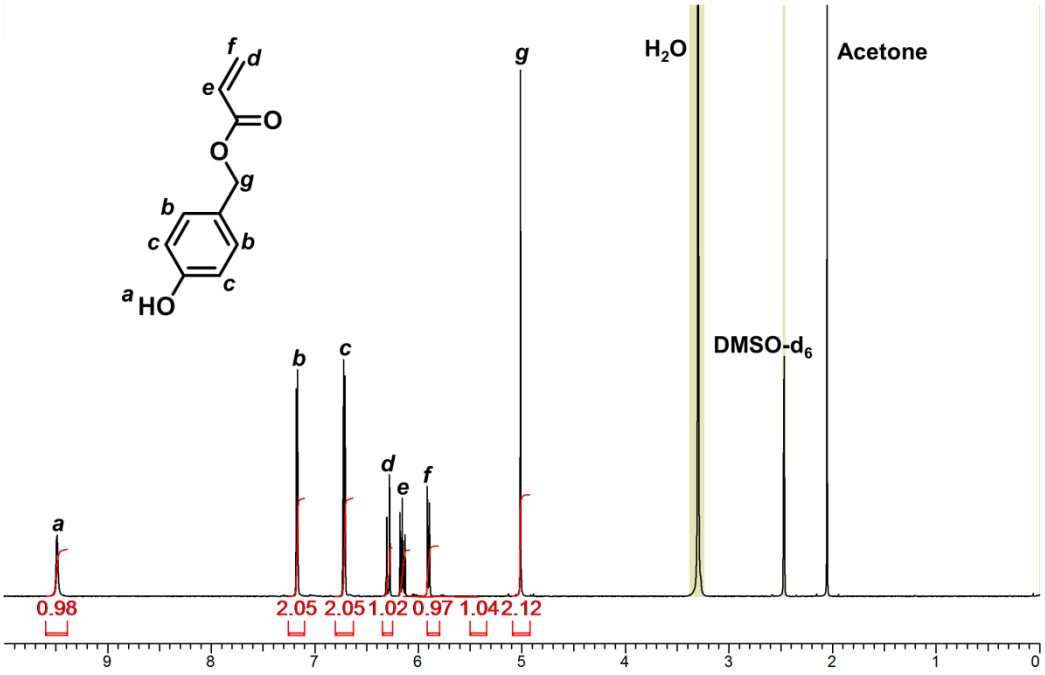

Supplementary Figure 2. ^{1}H NMR spectrum of P_2 in DMSO-d_6.

3-(3,4-dihydroxyphenyl)-2-hydroxypropyl acrylate (P_3). Triethylsilane-protected eugenol acrylate was synthesized, as described[2]. TBAF (1.71 ml, 1.71 mmol, 0.8 equiv) was added dropwise to a solution of the triethylsilane-protected eugenol acrylate (1 g, 2.14 mmol, 1.0 equiv) in THF (40 ml). After 1 hour stirring at room temperature, the crude material was purified via a silica gel flash column chromatography using methanol to remove triethylfluorosilane. Subsequently, the product was further purified by silica gel using 50 : 50 hexane/diethyl ether to provide 367 mg (90 % yield) of slightly brownish liquid.

^{1}H NMR (600 MHz, methanol-d_4): = 6.65 (d, 2H, Ar-*H*), 6.52 (q, 1H, Ar-*H*), 6.38 (d, 1H, -CH=CH_2), 6.15 (q, 1H, -C*H*=CH$_2$), 5.85 (d, 1H, -CH=CH_2) 4.09 (m, 3H, -C*H*(OH)CH_2OOC-), 2.75 (m, 2H, -CH_2CH(OH)-) (**Supplementary Fig. 3**). EI-MS, m/z = 238.08 [M+Na^{+}].

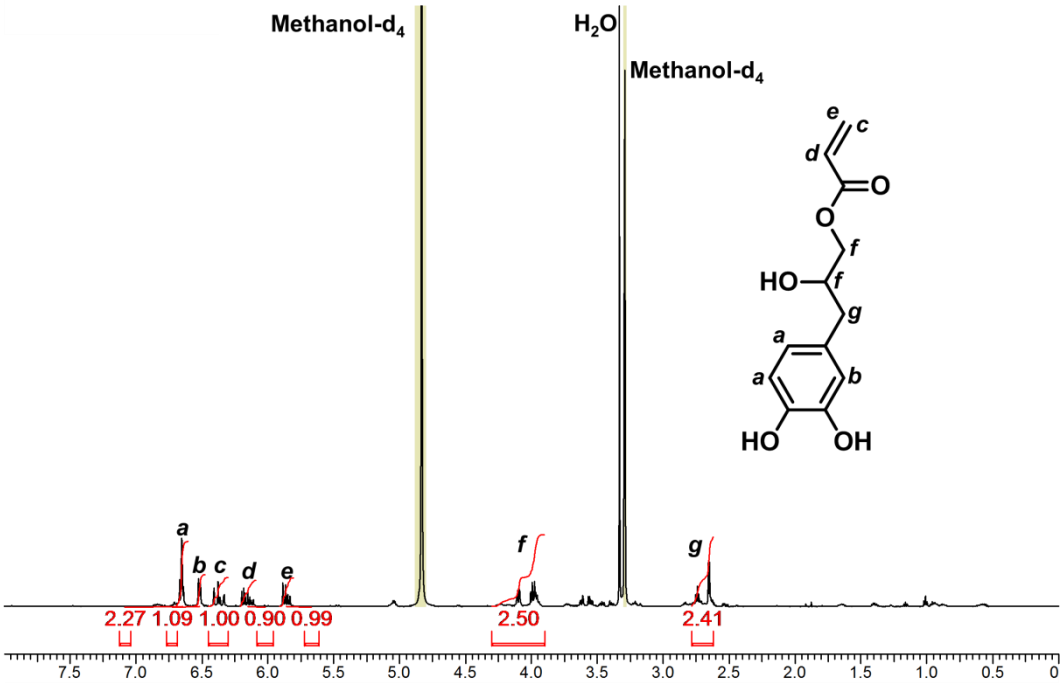

Supplementary Figure 3. ^{1}H NMR spectrum of P_3 in methanol-d_4.

8-((3-(3,4-dihydroxyphenyl)propanoyl)oxy)octyl acrylate (P_4). 1,8-Octanediol (16.7 g, 114.20 mmol, 2.5 equiv) and trimethylamine (7.6 ml, 54.71 mmol, 1.2 equiv) were agitated in THF (200 ml) at room temperature for 1 min. Subsequently, acryloyl chloride (3.7 ml, 45.59 mmol, 1.0 equiv) was added dropwise into the reaction mixture, and the reaction continued for 3 hours. The THF solvent was removed using a rotary vacuum evaporator. The crude material was extracted with 150 ml ethyl acetate and the solution washed with 1N HCl. After purification by Biotage Isolera^{TM} Prime automatic column chromatography (Biotage SNAP 50 g silica column; hexane/ethyl acetate 100 : 0 to 75 : 25 gradient; flow rate 40 ml/min), 4.03 g (44 % yield) of a transparent liquid (8-hydroxyoctyl acrylate) was obtained.

^{1}H NMR (600 MHz, $CDCl_3$): = 6.38 (d, 1H, -CH_2CH=CH_2), 6.10 (q, 1H, -CH_2CH=CH_2), 5.80 (d, 1H, -CH_2CH=CH_2), 4.13 (t, 2H, -CH_2CH_2OOC-), 4.07 (q, 2H, -CH(OH)CH_2OOC-), 3.63 (q, 2H, HO-CH_2CH_2-), 2.16 (s, 2H, HO-CH_2), 1.45 (m, 12H, -$CH_2CH_2CH_2CH_2CH_2CH_2CH_2$-).

3,4-Dihydroxyhydrocinnamic acid (2.75 g, 15.09 mmol, 0.75 equiv), DCC (4.15 g, 20.12 mmol, 1.0 equiv) and DMAP (2.46 g, 20.12 mmol, 1.0 equiv) were agitated in THF (200 ml) at room temperature for 1 hour. Subsequently, the 8-hydroxyoctyl acrylate (4.03 g, 20.12 mmol, 1.0 equiv) added into the reaction mixture, and the reaction continued for 3 hours. The THF solvent was removed using a rotary vacuum evaporator. The crude material was extracted with 150 ml ethyl acetate and the solution washed with 1N HCl. After purification by Biotage Isolera^{TM} Prime automatic column chromatography (Biotage SNAP 50 g silica column; hexane/ethyl acetate 100 : 0 to 50 : 50 gradient; flow rate 40 ml/min), 1.72 g (31 % yield) of a white crystal was obtained.

^{1}H NMR (600 MHz, DMSO-d_6): = 8.64 (q, 1H, Ar-*H*), 8.27 (d, 2H, Ar-*H*), 6.58 (d, 1H, -CH_2CH=CH_2), 6.53 (q, 1H, -CH_2CH=CH_2), 6.40 (d, 1H, -CH_2CH=CH_2), 3.98 (t, 2H, -COO-CH_2CH_2-), 3.55 (m, 4H, -CH_2CH_2OOC-, -CH_2-CH_2-OOC-), 2.62 (q, 2H, -ArCH_2CH_2-), 1.76-0.96 (m, 12H, -$CH_2CH_2CH_2CH_2CH_2CH_2CH_2CH_2$-) (**Supplementary Fig. 4**). EI-MS, m/z = 364.21 [M+Na^{+}].

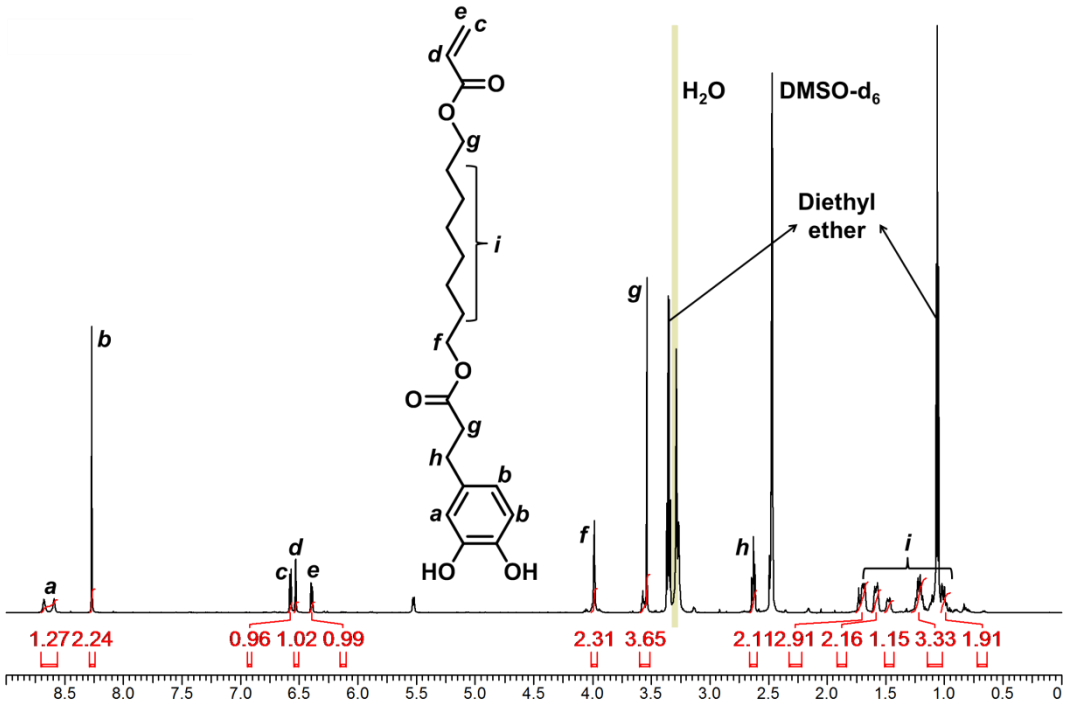

Supplementary Figure 4. ^{1}H NMR spectrum of P_4 in DMSO-d_6.

All solvents were degassed and filled with argon unless otherwise noted.

3. Atomic Force Microscopy (AFM) experiments

Each primer solution (1 wt%) was prepared in methanol (for P_1-P_3) or DMSO (for P_4). The primer solution was drop cast onto a freshly cleaved mica or glass surface, and kept at room temperature for 1 min. Subsequently, the surfaces were thoroughly rinsed with the respective solvents and dried with argon. All images, surface profiles and surfaces roughnesses were collected using an Asylum MFP-3D standard system (Asylum Research, Santa Barbara, CA) using silicon cantilevers (FORTGG-50, Applied NanoStructures, Santa Clara, CA) (**Fig. 1c** and **Supplementary Fig. 5**).

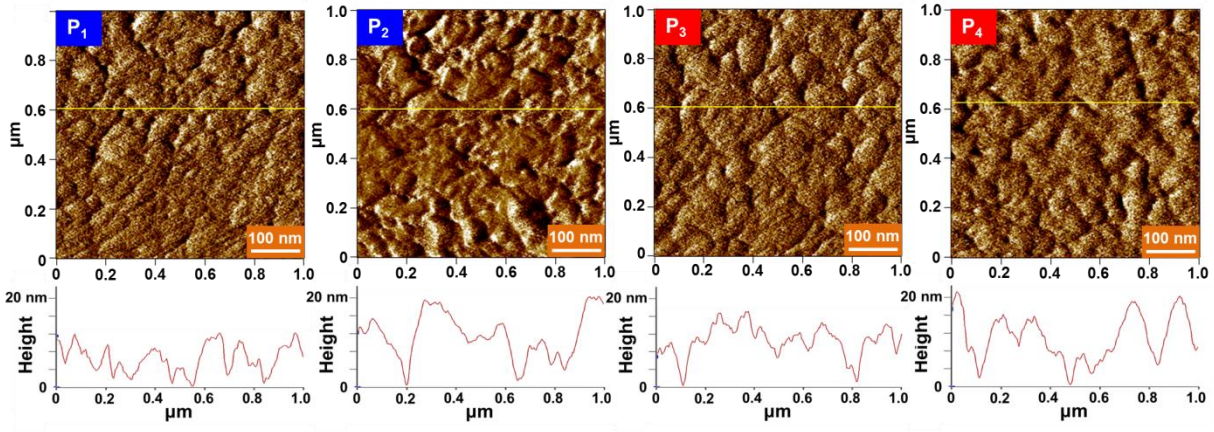

Supplementary Figure 5. AFM images and height profiles of adsorbed primers onto glass surfaces. The root mean square (RMS) roughness *R* of the glass is ~5 nm, making a quantitative comparison of the height profiles of the various primer-treated surfaces difficult, in contrast to results obtained using atomically smooth mica surfaces in which a clear comparison between the primed surfaces is possible (see main text). However, the general trends appear to follow those observed on the low-roughness mica substrates.

4. Quartz Crystal Microbalance with Dissipation (QCM-D) experiments

A 'static cell' (often called 'Open Module') QCM-D (Q-Sense, Biolin Scientific) was employed to quantitatively evaluate the adsorption of each primer onto SiO_2 surface using a quartz sensor (QSX 303, Biolin Scientific). Changes in resonance frequency (ΔF) and dissipation (ΔD) of the SiO_2 were recorded and used to measure the adsorbed mass and layer

viscoelasticity, respectively, of the primer deposited on the sensor. In detail, pure solvent (100 µl) was dropped onto the sensor and equilibrated for ~20-30 min. Then, 100 µl of a 2 wt% primer solution was dropped onto the sensor (this is labeled "Solution Drop-in" in **Supplemental Fig. 6**) and equilibrated until the frequency and dissipation signals stabilized. To remove unbound primers, the sensor was rinsed with solvents (this is labeled "Solvent Rinsing" in **Supplemental Fig. 6**) and equilibrated until frequency and dissipation signals stabilized.

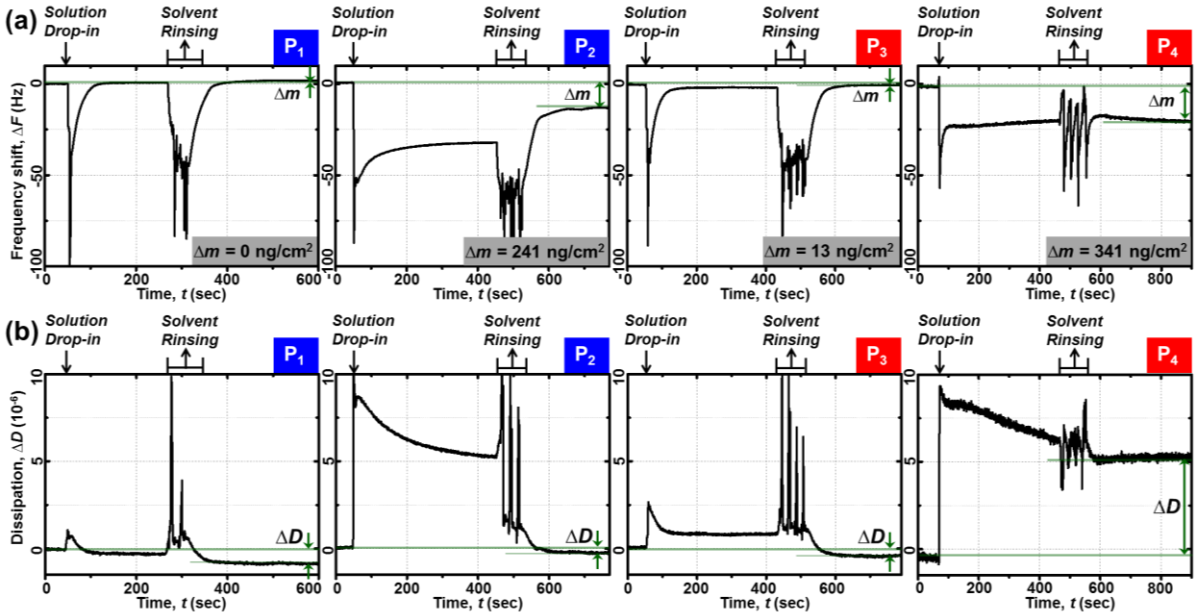

Supplementary Figure 6. (a) Frequency change (ΔF) and (b) dissipation change (ΔD) upon addition of each primer solution to a SiO_2 surface.

Given that the frequency change (ΔF) is proportional to the mass change (Δm) using the Sauerbrey equation[3], P_1, P_2, P_3, and P_4 adsorbed layers showed surfaces concentrations of 0, 241, 13, and 341 ng/cm^2, respectively. The calculated thickness of P_3 is ~1.2 nm, which agrees with height profile (~1-2 nm) obtained via AFM (P_3, **Fig. 1c**) and the contour length of P_3, demonstrating a conformal P_3 monolayer. Mass loss of P_3 and P_4 during the rinsing was negligible compared to P_2, which lost 60 % of initial mass, indicating outstanding adsorption efficiency of catechol-containing primers on SiO_2 surfaces even compared to mussel foot protein adsorption (~30 % loss of mfp-3s[4]). The priming thickness of P_4 estimated by QCM-

D is ~3.1 nm which agrees with the average layer height as obtained by AFM (~3.5 nm), assuming that QCM-D measures the average thickness of a uniform layer. The smaller average thickness of P_4 (~3.1 nm) compared to the molecular contour length (~4.8 nm) may be attributed to the flexible alkyl spacer in P_4. The possibility of P_4 forming a softer, more flexible layer as compared to other primers is supported by a higher change in dissipation (ΔD).

5. Molecular dynamics simulations

The models simulated by molecular dynamics (MD) consisted of a crystalline silica or mica slab and a layer of primer molecules embedded in a methanol box. The composition of each system and the final box size is shown in the **Supplementary Table 1**.

Supplementary Table 1 Description of simulated systems

Primer molecules		**Mineral surface**		**Solvent**		**Box size (nm)**		
type	**#**	**type**	**# atoms**	**type**	**# molecules**	**x**	**y**	**z**
P_1	180	Silica	17820	Methanol[5]	6990	8.10780	8.84410	10.46244
P_2	180	Silica	17820	Methanol[5]	6996	8.10780	8.84410	10.44390
P_3	180	Silica	17820	Methanol[5]	6786	8.10780	8.84410	10.37626
P_3	151	Mica[6, 7]	21504	Methanol[5]	5675	8.32320	7.21920	11.29101

All simulations were performed using the GROMOS 53A6 force field[8]. Parameters for primer molecules were derived from existing parameters for peptides and DPPC in the GROMOS 53A6 force field[8]. The charges for the catechol hydroxyl groups were estimated by a RESP fitting[9] from quantum level MP2/6-31G** within NWChem 6.1[10]. The obtained charges, 0.203 *e* for carbon; -0.626 *e* for oxygen and 0.423 *e* for hydrogen atoms were very similar to the ones already present for tyrosine in the above-mentioned force field.

To build the crystalline silica model, a unit cell was replicated filling a cube with approximate size of (8.1 x 8.8 x 3.1 nm). The silica surface was fully hydroxylated. The

following atomic charges were used for the silica: Si: 2.1 *e*, bulk O: -1.05 *e*, surface O: -0.950 *e* and H: 0.425 *e*.

The mica model used is a muscovite-2M$_1$, with formula $KAl_2(Si_3Al)O_{10}(OH)_2$[6]. The muscovite unit cell was replicated 16, 8 and 2 times along the *a*, *b* and *c* vectors, respectively. The crystal size was approximately (8.3 x 7.2 x 4.0 nm). Each mica surface contained a layer with one-half of adhered K^+ ions. The parameters used for this crystal model were obtained from the CLAYFF force field[7], which has been parameterized for the SPC water model[11], like the entire GROMOS 53A6 force field.

A. Starting structural framework. To obtain an appropriated density for the simulated systems, a box containing primer molecules and solvent was equilibrated by 1 ns of MD simulation. Then, the resulting system was placed onto the mineral surface to obtain the initial configuration for the molecular dynamics simulations.

The protocol to build the box with solvent and primer molecules is described below. Multiple primer molecules were randomly distributed as a dense layer along the *x*-*y* plane. These molecules were built in an extended configuration with their phenyl groups along the mineral normal plane, so that they would be oriented towards the mineral surface upon building the initial system. The systems were placed in a rectangular simulation box about 1.5 nm away from the mineral surfaces. The box lengths were the same size as the mineral surfaces in *x* and *y* directions and the *z*-axis length was 7.8 nm. The solute boxes were solvated using a methanol[5] solvent model, and the number of primer molecules and solvent molecules added is shown in **Supplementary Table 1**.

An initial energy optimization was obtained using 10,000 steps of the steepest descent algorithm. Simulations were performed for 1 ns in a NPT ensemble using semi-isotropic conditions. Reference pressure used was 1 bar coupling each 0.5 ps via a Berendsen's barostat[12]. The pressure coupling was isotropic in the *x* and *y* directions with compressibility

set to zero, while in *z* direction the compressibility was set to 7.5×10^{-4} bar^{-1}. The LINCS algorithm[13] was used to constrain all bonds in methanol systems with a 2 fs integration time step. Integrations were carried out by the leapfrog algorithm[14]. Periodic boundary conditions in the *x, y* and *z* directions were applied to all systems. A cutoff radius of 1.4 nm was used to compute the short-range electrostatics and van der Waals interactions, updating the neighbor list each 5th step. Electrostatic interactions outside of the 1.4 nm cutoff sphere were treated using the reaction field method[15] with ε = 32.63 for methanol. The velocity rescale scheme[16] kept the temperature at 300 K with a time coupling of 0.1 ps. The initial velocities were generated randomly according to a Maxwell distribution at 300 K. Center of mass translation was removed at every step. The simulations were performed using the GROMACS 4.6.x simulation package[17].

After each simulation of solvent and primer molecules the resulting systems were placed onto their respective mineral surface, the final box sizes are shown in **Supplementary Table 1**. A new energy optimization was carried using the steepest descent algorithm of 10,000 steps.

B. Production. Simulations were performed for 500 ns with the NVT ensemble. Periodic boundary conditions were used in all directions. The position for the mineral bulk atoms was constrained in *x, y* and *z* dimensions during the simulations. The aforementioned constraint was not applied to hydrogen atoms from the hydroxyl groups and K^+ ions in the mica surface. LINCS method[13] was used to constrain all bonds and a 2-fs time step integration used. Integrations were carried out by the leapfrog algorithm[14]. A cutoff radius of 1.4 nm was used to compute the short-range electrostatics and van der Waals interactions, updating the neighbor list each 5th step. Electrostatic interactions outside of the 1.4 nm cutoff sphere were treated using Particle-mesh Ewald (PME) method[18]. The velocity rescale scheme[16] kept the temperature at 300 K with a coupling time of 1 ps. The velocities were generated randomly

according to a Maxwell distribution at 300 K. Center of mass translations were removed at every step. The simulations were performed using the 4th versions of GROMACS simulation package[17].

In support of the results outlined in the main text, additional analyses are presented below for the primer molecule simulations. P_2 molecules showed strong interaction with silica surface, however the higher diffusion coefficient along the *z* direction (perpendicular axis to the mineral surface) indicated the lower propensity for efficient adhesion (**Supplementary Table 2**). In addition, P_2 molecules also showed a higher diffusion coefficient in the *x-y* plane as compared to P_3 molecules. P_1 molecules showed high translational mobility on *x-y* plane, but lowest mobility in the *z* direction (normal to the mineral) as a consequence of the confinement between surfaces on which they presented weak affinity.

Supplementary Table 2 Diffusion coefficient along the *z* axis and in the *xy* plane

	***z* axis** (10^{-7} cm^2 s^{-1})	***xy* plane** (10^{-5} cm^2 s^{-1})
P_1	0.01855	1.7497
P_2	2.19	0.6463
$P_{3\ silica}$	1.74	0.0174
$P_{3\ mica}$	1.63	0.3374

6. Preparation of Silane-grafted substrates[19]

Freshly cleaved mica and clean glass slides were placed in a desiccator (Pyrex nalge Sybron Corp) with a small dish of 3-(trimethoxysilyl)propyl acrylate (200 µl). The desiccator was evacuated for 30 min and then sealed to allow the silane deposition to occur overnight at room temperature. The surfaces were then rinsed with ethanol and dried with argon.

7. Statistical analysis

All data of the adhesion and mechanical testing results in this article are given as the mean and ± standard deviation. The Student's *t*-test was used to confirm the significance of the comparison. *P* values of less than 0.05 are considered to be significantly different.

8. Lap shear tests

1 wt% primer solution was spread on mica, glass, tooth enamel, or a silicon wafer and incubated for 1 min, followed by thorough washing with methanol (for MDP, P_1-P_3) or DMSO (for P_4) and drying by flowing nitrogen. The surfaces were exposed to a basic aqueous solution (pH 9, using sodium hydroxide), incubated for 1 min, and dryed by flowing nitrogen (see **Supplementary Fig. 7**). The methacrylic comonomer blend (Bis-GMA, TEGDMA, DMAEMA and CQ) was packed in a gelatin capsule (size #4, 5-mm diameter, Torpac Inc.) and placed up on top of the primer-treated substrates. The comonomer blend was cured (or crosslinked) for 1 min using a portable dental curing lamp (Foshan Liang Ya Dental Co., LY-A180, 420-480 nm, 1200-2000 $mW \cdot cm^{-2}$) (see **Supplementary Fig. 8**). Uniaxial compression was applied to the capsule at a rate of 0.05 inch min^{-1} using a materials testing system (MTS Bionix 200) until the capsules separated from the substrate. The lap shear fracture measurements were repeated at least 10 times for each condition.

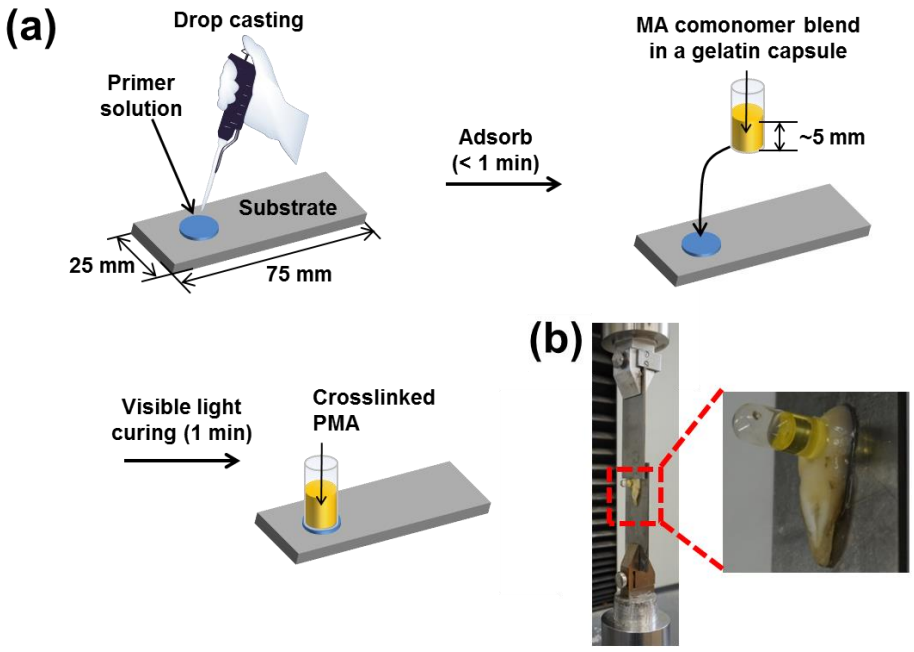

Supplementary Figure 7. Schematic of sample preparation for the lap shear test. (b) Photograph of experimental setup for the lap shear measurement of crosslinked PMA on the surface-treated tooth enamel.

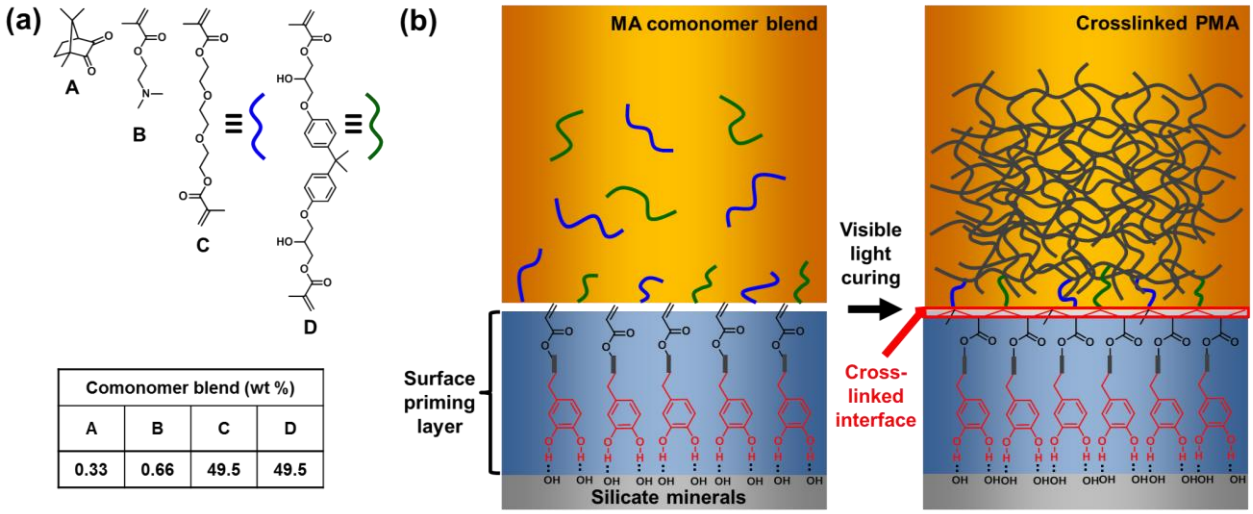

Comonomer blend (wt %)			
A	B	C	D
0.33	0.66	49.5	49.5

Supplementary Figure 8. (a) Comonomer composition of a visible light-curable methacrylic adhesive blend — camphorquinone, comonomer A, 2-(dimethylamino)ethyl methacrylate, comonomer B, triethylene glycol dimethacrylate, comonomer C, and bisphenol A glycerolate dimethacrylate, comonomer D. (b) Schematic drawing showing the polymerization and crosslinking of the PMA onto a catechol-primed surface.

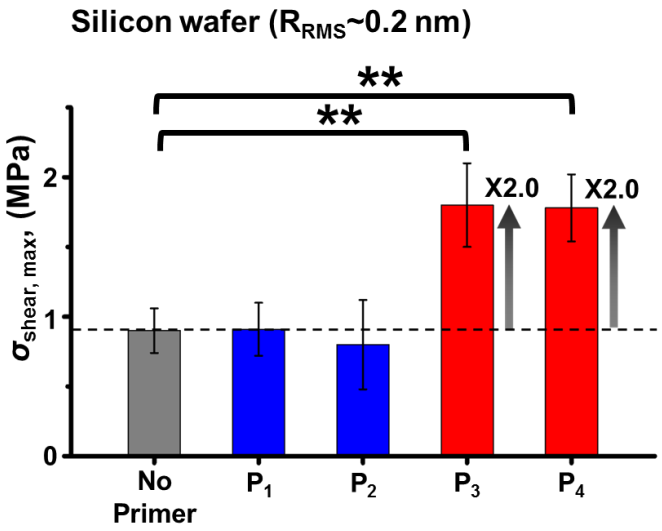

Supplementary Figure 9. Lap shear strength of cured PMA on silicon wafer surfaces treated with different primers (P_1, P_2, P_3 and P_4). *P*-values were calculated using the Student's *t*-test; $^{**}p<0.001$

9. Surface Forces Apparatus (SFA) experiments

Atomically-smooth muscovite mica sheets were freshly cleaved (thickness of 2-5 μm) and attached on another large freshly cleaved mica backing sheet in a laminar flow hood and then placed in a desiccator for clean storage. To ensure use of a fresh surface for each experiment, mica was peeled away from the backing sheet and glued on cylindrical disks using an epoxy glue (EPON 1004 F® from Exxon Chemicals)[20]. In each experiment, the mica surfaces were treated with one of the primer solutions, as described for the lap shear experiments, and then mounted in the SFA in a cross cylindrical geometry. In contrast to typical SFA experiments, which use an interferometric method to calculate the disk-disk separation distances and thus the interaction forces[21], in the SFA used here for adhesion testing, the disk separations were directly measured using semiconductor strain-gauged double cantilever springs[2, 22] (*k*=1000-10000 N/m) (see **Supplementary Fig. 10**). After separating the surfaces, 100 μl of comonomer blend was injected between the two surfaces. Then, ~600 mN of load was applied, followed by visible light curing for 1 min using the portable dental curing lamp (see **Figure 3g**). The adhesion strength of the cured polymer to the mica was measured by

detaching (unloading) the two surfaces. All loading and unloading was performed using a coarse micrometer at a velocity of ~2 mm s^{-1}. The SFA measurements were repeated at least 5 times for each condition.

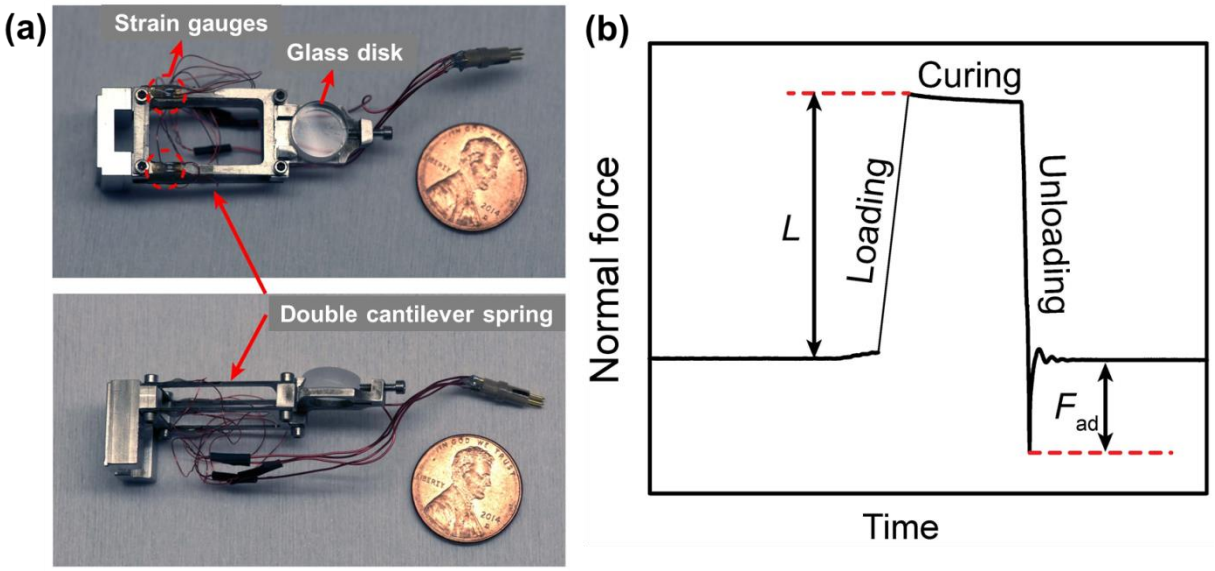

Supplementary Figure 10. (a) Photograph of strain gauge attached double cantilever spring, which allows direct measurement of forces in the SFA. (b) An example of the measured normal force signal during loading and adhesion force measurement.

To enable comparison of the SFA data with measurements of native mussel adhesives, the adhesion pressure of the actual mussel plaques was calculated as follows. The critical force for detachment of a ~3-mm diameter plaque under conditions of purely adhesive failure was measured to be ~ 2 N[23]. The adhesive pressure can be crudely estimated by dividing this critical force by the adhesive area ~ π (1.5 mm)^2) = 272 kPa.

10. Cell viability assays on surface treated glasses[24]

L929 mammalian fibroblast cells were purchased from the Korean Cell Line Bank (Seoul, Korea) and cultured in Roswell Park Memorial Institute (RPMI) 1640 media (Life Technologies) with 10 % fetal bovine serum (Gibco), 25 mM sodium bicarbonate and 1% penicillin−streptomycin (Gibco). Silane-grafted and Catechol (P_3) primed glass slides were prepared by following procedures described in sections 6 and 3, respectively. Each glass

substrate was placed on the 100π (the size of the cell culture plate) cell culture plate and sterilized by addition of a 70% ethanol solution. After equilibration in phosphate buffered saline (PBS) and media for 5 min each, L929 cells were seeded onto the glass substrates at a density of 1×10^6 cells per plate. Cells were incubated for 3 days in 5% CO_2 at 37 ºC. After 3 days, the substrates were transferred to new culture plates and washed extensively with PBS. Cells were then detached by 0.05 % trypsin-EDTA and stained with trypan blue solution to assess cell viability. Living cells are impermeable to the stain, whereas dead cells with compromised membranes turn blue. The number of live cells was counted using a standard hemocytometer. The bare glass slide without any modification served as a control (**Supplementary Fig. 11**).

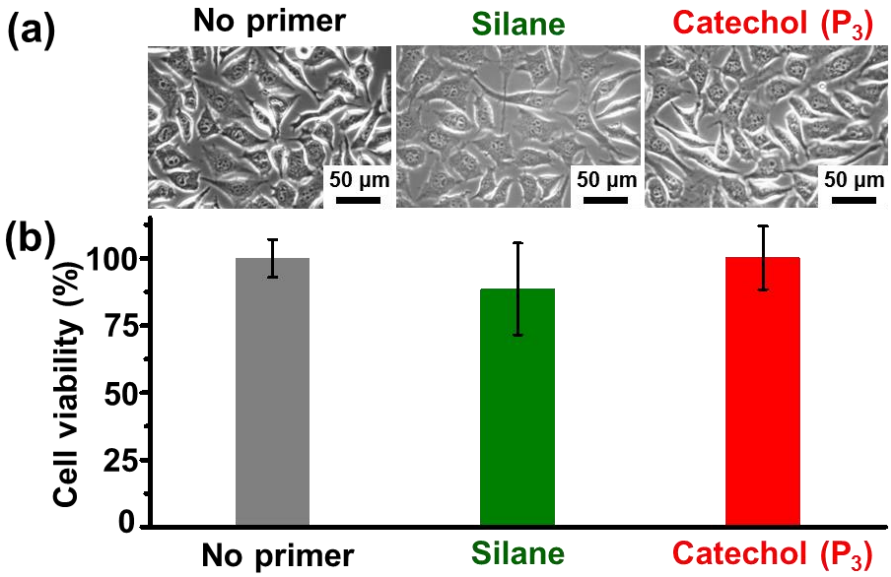

Supplementary Figure 11. (a) Phase-contrast microscopy images and (b) cell viability results of L929 mammalian fibroblast cells grown on untreated glass slides ('no primer') or glass slides treated with Silane or Catechol (P_3) primer. Each bar represents the average cell viability from 9 different glass slides, and the error bars indicate standard deviation.

11. Preparation of surface-treated glass fillers

A. Silane-grafted glass filler[25]. To a solution of deionized water (70 ml) and ethanol (30 ml), 3-(trimethoxysilyl)propyl acrylate (0.5 g) and 1N acetic acid (0.125 ml) was added sequentially. The mixture was vigorously stirred for 1 hour at room temperature. 5g of the

non-treated glass filler (Youth Tech Co.) was gradually added to the solution and vigorously stirred for 2 hours. The slurry was precipitated (or rinsed) by centrifugation at 10,000 rpm for 5 min. The rinsing procedure was repeated three times. The precipitate was dried in a freeze drier for 48 hours. The dried filler was placed in a drying oven at 120 ^{o}C for 2 hours to complete the silane grafting reaction.

B. Catecholic primer (P_3)-treated glass filler. To a 1 wt% P_3 solution in methanol (25 ml), the non-treated glass filler (5 g) was gradually added and vigorously stirred for 10 min at room temperature. The slurry was rinsed by centrifugation at 10,000 rpm for 5 min. The rinsing procedure was repeated three times. The precipitate was dried in a freeze drier for overnight. The dried filler was gradually added to pH 9 aqueous solution and vigorously stirred for 10 min. The slurry was rinsed three times by centrifugation at 10,000 rpm for 5 min. The precipitate was dried in a freeze drier for 48 hours.

12. Compression tests of composites

To the comonomer blend in agate mortar (Walter Stern Inc.), the surface-treated glass fillers were thoroughly mixed using a pestle at 80 ^{o}C (Note: the glass fillers were filtered with a 60 standard mesh using a Mini-Sieve^{TM} micro sieve set (Sigma-Aldrich) prior to mixing with the comonomer blend). The mixture was drawn into a 1-ml syringe (BD), completely filling it, then cured for 3 min using the portable dental curing lamp. The cured PMA composites were then cut into cylinderical specimens (4.6 mm diameter, 10 mm height). Uniaxial compression was applied to the specimen at a rate of 1 mm min^{-1} using a materials testing system (Instron 8871) at room temperature.

A. Steady-state failure tests. The composite specimens were compressed until the specimens failed by fragmentation. The compressive failure measurements were repeated for at least 8 specimens. In the analysis of the stress-strain curve (**Fig. 4b**), the zero strain value was found by linear extrapolation of the elastic regime. The toughness values were

determined using an 8th order polynomial fit to smooth and approximate the data. The fit curve was then integrated to to avoid the complications of non-uniform and non-monotonic strain values. The ultimate strength was given as the maximum stress recorded for each sample. The strain at failure is given by the strain value at which the maximal stress occurred.

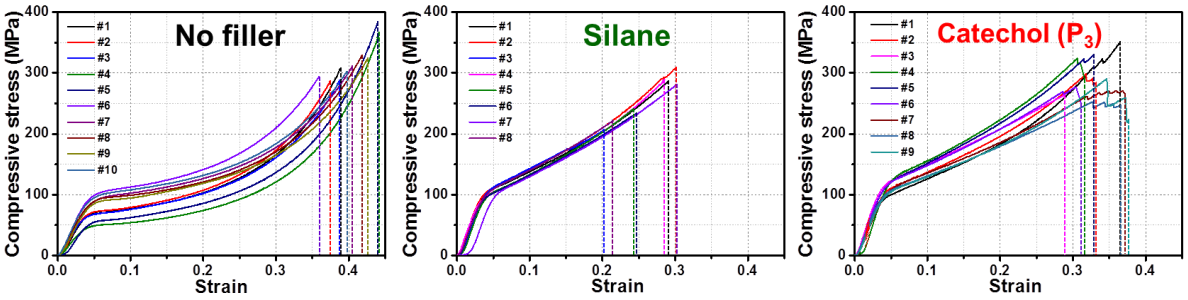

Supplementary Figure 12. Stress-strain curves of the unfilled PMA composites, Silane-treated glass-filled PMA composites, and P_3-coated glass-filled PMA composites.

13. Dynamic thermo-mechanical tests

The mineral-PMA composites were prepared by curing the mixture (comonomer blend and glass fillers) within a Teflon mold (8 mm diameter, 0.5 mm thickness). The mechanical properties were measured using an ARES-LC rheometer (Rheometric Scientific) in a 8-mm-diameter parallel plate geometry at 175 ^{o}C (above the glass transition temperature, T_g ~156 ^{o}C, of the composites). Strain sweeps were conducted at ω=0.1 Hz. Frequency sweeps were performed from ω=10 Hz to 0.1 Hz at strain amplitude of γ_0=0.1% and 1%, which lie within the linear viscoelastic region of our materials. The measured trends for the storage shear moduli (G') of the composites ($G'_{Silane} \approx G'_{Catechol} > G'_{no\ fillers}$) generally agreed with the elastic modulus (E) measured in the compressive failure test (**Supplementary Fig. 13**). Note: Strain sweep experiments determined the linear viscoelastic region (0.1-1 % strain) before running the frequency sweep. The loss moduli (G") measurements were unreliable due to extremely high stiffness of the composites, and are not reported.

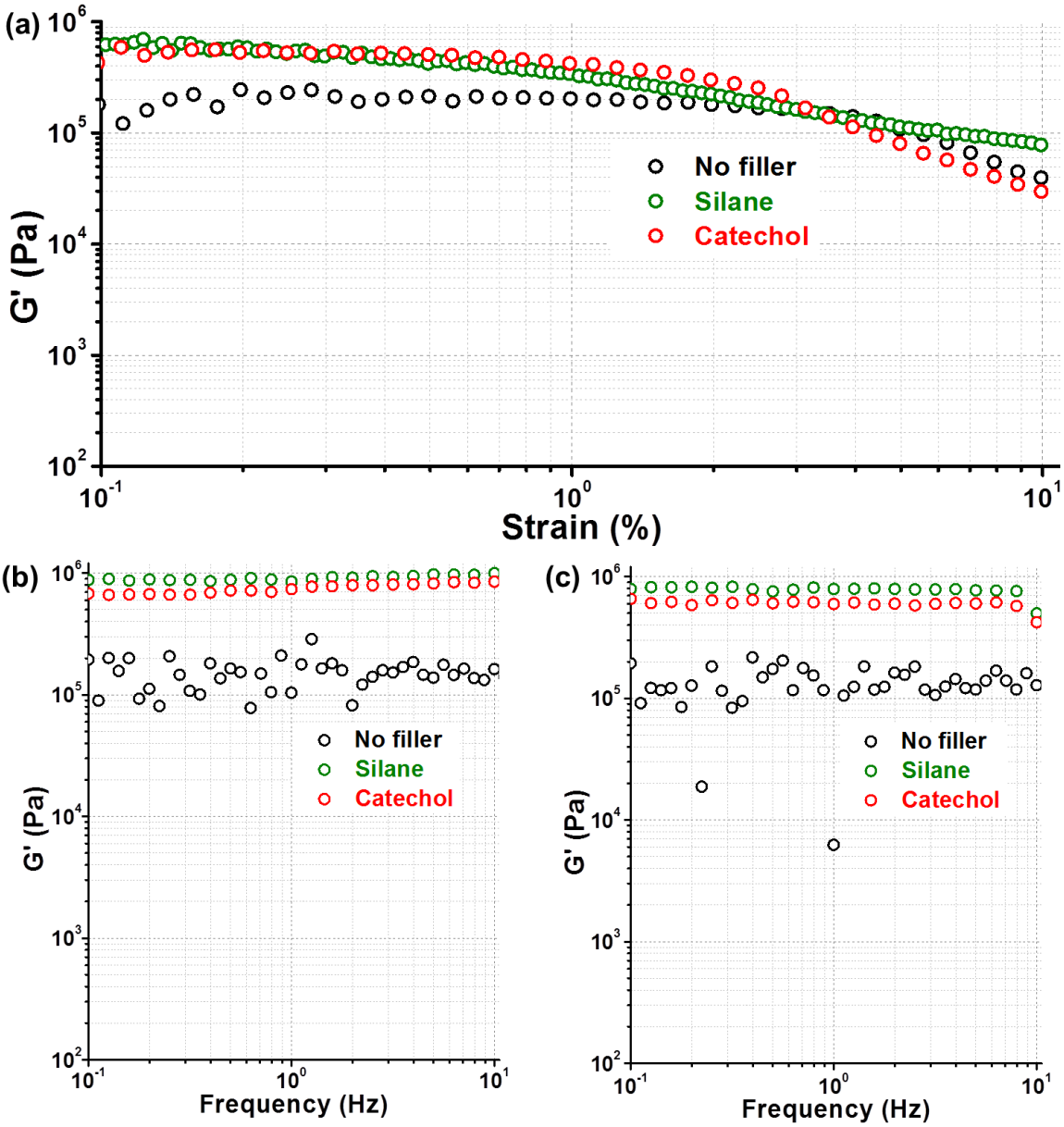

Supplementary Figure 13. (a) Storage moduli (G') as a function of strain amplitude for the unfilled PMA resin and primer-treated glass-filled PMA composites. Frequency sweep of the composites at (b) 0.1 % and (c) 1 % strain (both within the linear range). The loss modulus was too small to be reliably measured.

14. Scanning Electron Microscope (SEM)

For imaging of samples before compressive failure, samples were polished using a 1-µm diamond slurry to allow for analysis of the filler distribution and identify any voids that might exist within the composite. After compressive failure, pieces of the fracture debris were directly imaged without any treatment to determine the location of failures. In all cases, the samples were sputter coated with gold/palladium 60/40, 99.99% (Hummer 6.2, Anatech) for

90 s and imaged in secondary electron mode with a scanning electron microscope (FEI XL30 Sirion FEG) (**Supplementary Fig. 14**).

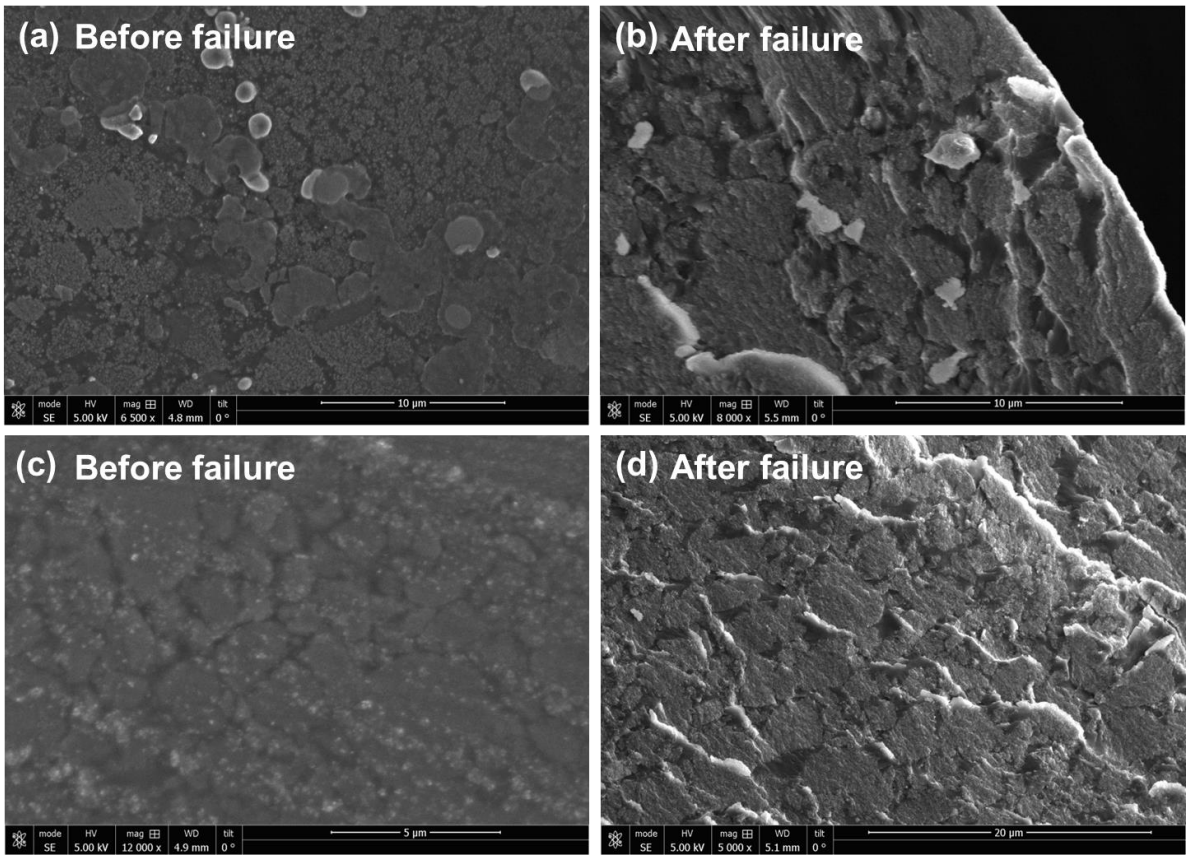

Supplementary Figure 14. SEM images of (a, b) Silane-treated glass-filled composite (c, d) Catechol-treated glass-filled containing composite before (left column) and after (right column) compressive failure.

15. Thermal analysis

Thermogravimetric analysis (TGA) and Differential Scanning Calorimetry (DSC) of the composites were performed using a Discovery TGA (TA instruments) and Q2000 DSC (TA instruments), respectively, with nitrogen as the purging gas. In the both experiments, the heating rate was 10 ^{o}C/min. Silane- and Catechol-coated glass-filled PMA composites showed very similar thermogravimetric curves (**Supplementary Fig. 15**).

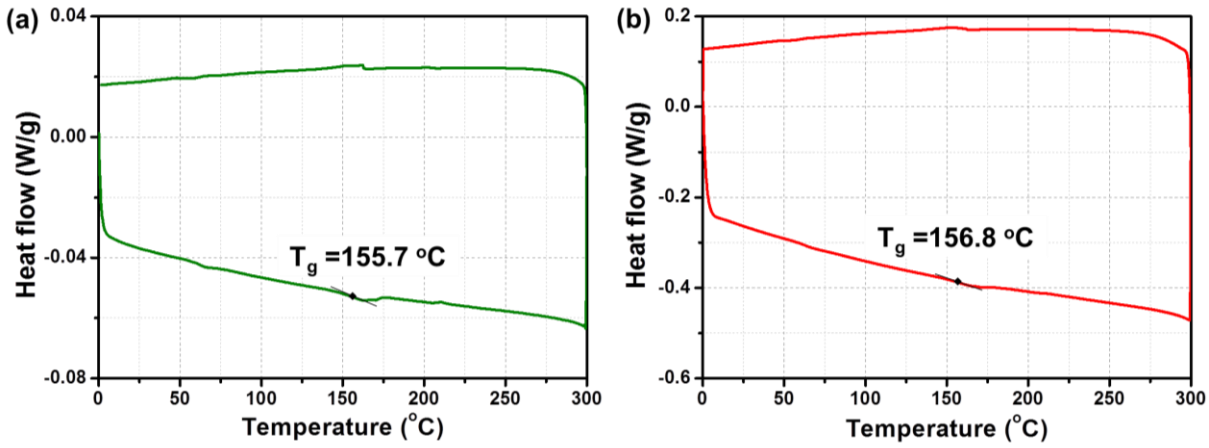

Supplementary Figure 15. Differential scanning calorimetry curves of (a) Silane-treated glass-filled composite and (b) Catechol-treated glass-filled composite.

After complete thermal decomposition of organic compounds, TGA curves exhibits ~30 wt% of inorganic compounds, the glass transition temperatures (T_g) shown in TGA (no filler – ~155 °C, Silane – ~156 °C, Catechol – ~156 °C) are similar to DSC results (**Supplementary Fig. 16**).

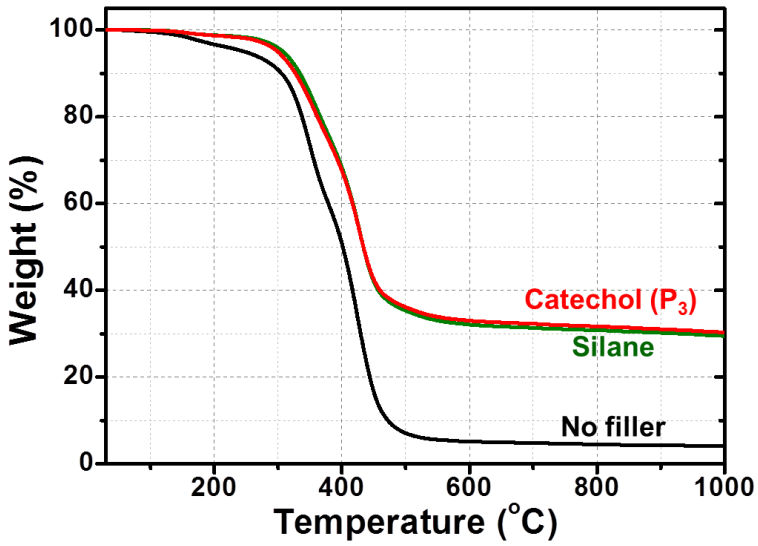

Supplementary Figure 16. Thermogravimetric curves of the unfilled PMA resin and primer-treated glass-filled PMA composites.

Supplementary References

[1] G. E. Fantner, T. Hassenkam, J. H. Kindt, J. C. Weaver, H. Birkedal, L. Pechenik, J. A. Cutroni, G. A. G. Cidade, G. D. Stucky, D. E. Morse, P. K. Hansma, Nat Mater 2005, 4, 612; C. K. C. Lieou, A. E. Elbanna, J. M. Carlson, Physical Review E 2013, 88, 012703.
[2] B. K. Ahn, D. W. Lee, J. N. Israelachvili, J. H. Waite, Nat Mater 2014, 13, 867.
[3] G. Sauerbrey, Z. Physik 1959, 155, 206.
[4] W. Wei, Y. Tan, N. R. Martinez Rodriguez, J. Yu, J. N. Israelachvili, J. H. Waite, Acta Biomaterialia 2014, 10, 1663.
[5] R. Walser, A. Mark, W. van Gunsteren, M. Lauterbach, G. Wipff, Journal of Chemical Physics 2000, 112, 10450.
[6] A. Dequidt, J. Devemy, P. Malfreyt, Journal of Physical Chemistry C 2015, 119, 22080.
[7] R. Cygan, J. Liang, A. Kalinichev, Journal of Physical Chemistry B 2004, 108, 1255.
[8] C. Oostenbrink, A. Villa, A. E. Mark, W. F. Van Gunsteren, Journal of Computational Chemistry 2004, 25, 1656.
[9] C. I. Bayly, P. Cieplak, W. Cornell, P. A. Kollman, The Journal of Physical Chemistry 1993, 97, 10269.
[10] M. Valiev, E. J. Bylaska, N. Govind, K. Kowalski, T. P. Straatsma, H. J. J. Van Dam, D. Wang, J. Nieplocha, E. Apra, T. L. Windus, W. A. de Jong, Computer Physics Communications 2010, 181, 1477.
[11] H. J. C. P. Berendsen, J. P. M.; van Gunsteren, W. F.; Hermans, J., in *Intermolecular Forces*, (Ed: B. Pullman), Reidel, Dortrecht 1981, 331.
[12] H. J. C. Berendsen, J. P. M. Postma, W. F. van Gunsteren, A. DiNola, J. R. Haak, The Journal of Chemical Physics 1984, 81, 3684.
[13] B. Hess, H. Bekker, H. J. C. Berendsen, J. G. E. M. Fraaije, Journal of Computational Chemistry 1997, 18, 1463.
[14] R. W. Hockney, in *Methods in Computational Physics*, Vol. 9 (Eds: B. Alder, S. Fernbach, M. Rotenberg), Academic Press, New York/London 1970.
[15] I. G. Tironi, R. Sperb, P. E. Smith, W. F. van Gunsteren, The Journal of Chemical Physics 1995, 102, 5451.
[16] G. Bussi, D. Donadio, M. Parrinello, The Journal of Chemical Physics 2007, 126, 014101.
[17] B. Hess, C. Kutzner, D. van der Spoel, E. Lindahl, Journal of Chemical Theory and Computation 2008, 4, 435.
[18] U. ESSMANN, L. PERERA, M. BERKOWITZ, T. DARDEN, H. LEE, L. PEDERSEN, Journal of Chemical Physics 1995, 103, 8577.
[19] C. Pick, C. Argento, G. Drazer, J. Frechette, Langmuir 2015, 31, 10725; N. R. Glass, R. Tjeung, P. Chan, L. Y. Yeo, J. R. Friend, Biomicrofluidics 2011, 5, 036501.
[20] J. Israelachvili, Y. Min, M. Akbulut, A. Alig, G. Carver, W. Greene, K. Kristiansen, E. Meyer, N. Pesika, K. Rosenberg, H. Zeng, Reports on Progress in Physics 2010, 73, 036601; J. N. Israelachvili, 2010, 227.
[21] D. W. Lee, X. Banquy, K. Kristiansen, Y. Kaufman, J. M. Boggs, J. N. Israelachvili, Proceedings of the National Academy of Sciences 2014, 111, E768.
[22] D. W. Lee, X. Banquy, J. N. Israelachvili, Proceedings of the National Academy of Sciences 2013, 110, E567.
[23] K. W. Desmond, N. A. Zacchia, J. H. Waite, M. T. Valentine, Soft Matter 2015, 11, 6832.
[24] ISO 10993-1:2009.
[25] J.-H. Lee, C.-M. Um, I.-b. Lee, Dental Materials 2006, 22, 515.